



Supporting Online Material for
The Latitudinal Distribution of Clouds on Titan

P. Rannou,* F. Montmessin, F. Hourdin, S. Lebonnois

*To whom correspondence should be addressed. E-mail: pra@aero.jussieu.fr

Published 13 January 2006, *Science* **311**, 201 (2006)
DOI: 10.1126/science.1118424

This PDF file includes:

Materials and Methods

Figs. S1 and S2

Table S1

References

Support online material

Materials and methods

To investigate the origin of clouds on Titan in a self consistent way, we have coupled a cloud microphysical model to a general circulation model (GCM) (1). The circulation model is a latitude-altitude (48 latitude points and 55 altitude levels) restriction of a three-dimensional model (2) where the equations of meteorology are solved numerically. The latitudinal transport by barotropic waves in the stratosphere, not explicitly calculated in the two-dimensional model, is parametrized as a horizontal diffusion (3). In our model, aerosol production is proportional to the solar insolation and occurs at about 400 km. The global annual-averaged production rate is $1.2 \times 10^{-12} \text{ kg m}^{-2} \text{ s}^{-1}$. Aerosols grow, settle and are transported by winds. Haze and wind interaction produces several marked latitudinal contrasts in the haze distribution (1). In return, the haze absorbs the light and acts on the winds by modifying the thermal structure, causing a strong feedback between haze and winds (4). The cloud scheme, adapted from a Mars water ice cloud model (5), uses the laws of the microphysics (6). The parameters for the phase changes of methane and ethane and other important parameters are given in Table S1. We consider ethane because it is the most abundant byproduct of the photochemical destruction of methane and nitrogen. But, other chemical species produced by photochemistry condense on Titan in locations similar to ethane, and become mixed with the ethane clouds. The methane source is deduced from a simple evaporation flux law which forces the saturation ratio to be about 50% everywhere at the surface (Fig. 2b). Ethane source is prescribed by a mass production rate uniform in latitude at the top of the model. The production rate is set to obtain a ethane mixing ratio of about 1.2×10^{-5} in the stratosphere. Droplet formation is initiated by nucleation onto aerosols and is followed by condensation or evaporation depending on thermodynamic conditions. Aerosols on which condensation occurs become cloud nuclei and are no more counted as aerosols but as nuclei. In this way, clouds can affect the haze distribution. The aerosol distribution is discretized with 10 size-bins between $1.64 \times 10^{-9} \text{ m}$ and about $6.7 \times 10^{-6} \text{ m}$ (aerosol volume increases by a factor of 16 between two adjacent bins). The cloud nuclei distribution is also described with the same 10 bins. The ethane and methane condensed phases are specified by the total volume of both species deposited on the nuclei of each bins. Then the volume of the drops, for one given nuclei bin, is obtained by dividing the total volume of condensate (ethane plus methane) by the number of nuclei in this bin. Drops can be made of both types of condensates simultaneously. Drops are supposed to be spherical, and the possible effect of condensate mixing is not accounted for. Then, no distinction is done here between solid and liquid condensed phases. Clouds are transported by winds and radiative feedback is also accounted for. In contrast, the distribution of gaseous species is prescribed for radiative transfer calculations. Drops are supposed to be perfectly spherical for sedimentation. Cloud optical properties are derived from Mie theory using predictions for both drop concentration and radius. Drop refractive indices are weighted according to liquid methane, ethane and tholin (7, 8) refractive indices. Thermodynamic feedback due to latent heat release is also included, but is found to be negligible. Finally, to compute the surface temperature, we use a simple temperature model based on Fick's diffusion law discretized with 10 layers. Since the internal temperature is not needed, only the thermal inertia is specified.

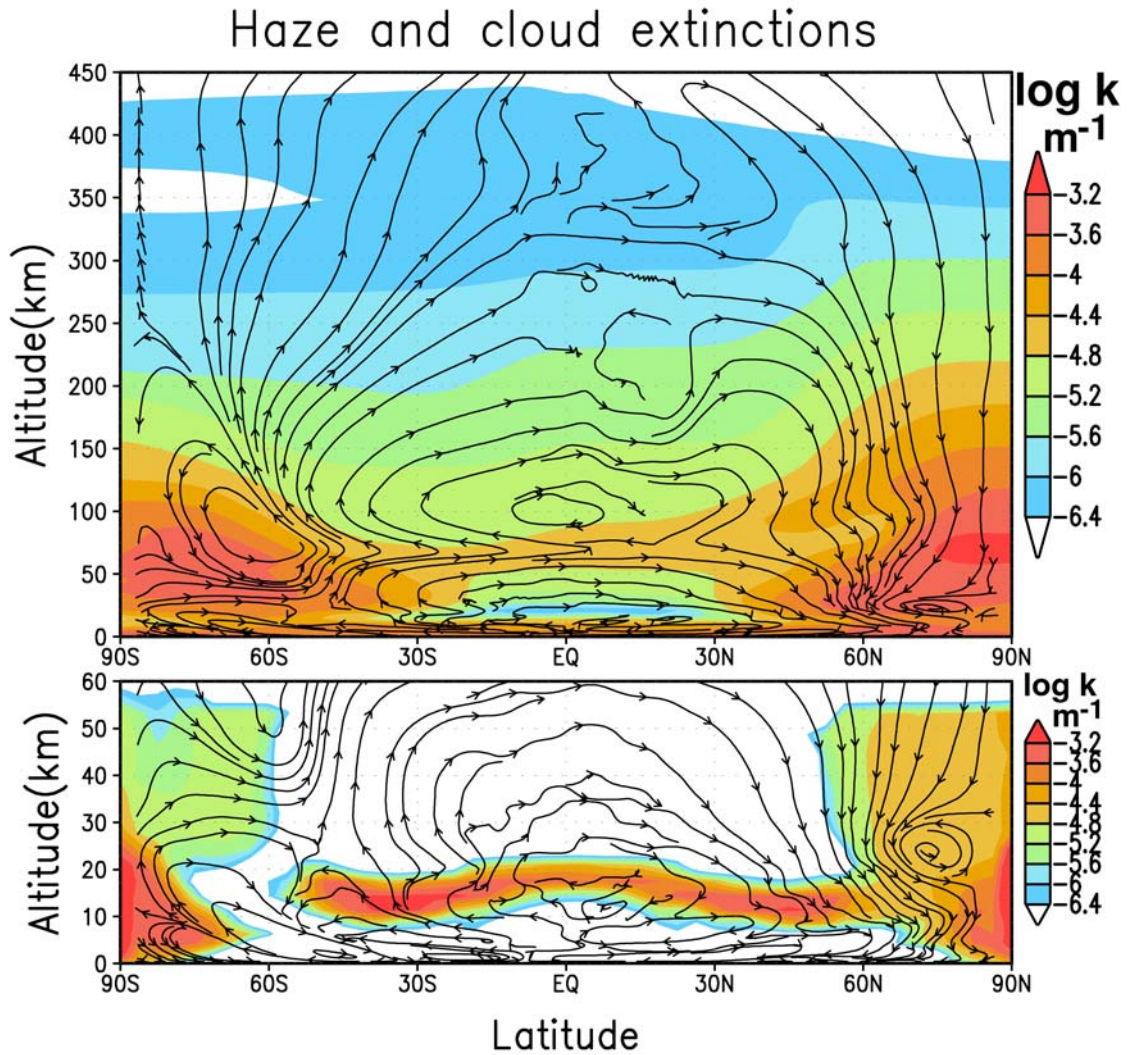


Figure S1 Haze (upper panel) and cloud extinction (bottom panel) shown along with the direction of the winds. For each panel, extinctions and winds are averaged over 1 terrestrial year before Cassini/Huygens arrival time. Note that averaging the cloud extinction produces a rather homogeneous and continuous plot between $\pm 60^\circ$ whereas clouds are actually patchy and sporadic. In the haze extinction panel, we can see the detached haze layer, the north and south polarhoods, and the haze asymmetry between the northern (between equator and $50^\circ N$) and southern hemisphere (between $50^\circ S$ and equator). The cloud and aerosol interaction produces a new feature: the strong haze removal in the troposphere (near 20 km between $40^\circ S$ and $40^\circ N$ and at 10 km in polar regions). The cloud extinction panel shows a cloud layer, essentially made of methane, between 10 and 20 km altitude at latitudes between $50^\circ S$ and $50^\circ N$. In polar regions, a widespread cloud of ethane is located poleward to $\pm 60^\circ$ latitudes and below 60 km altitude. At lower altitudes, and very close to the pole (latitude poleward to $\pm 80^\circ$) a thick methane cloud exists below 20 km, but can sometimes reach altitudes up to 30 km.

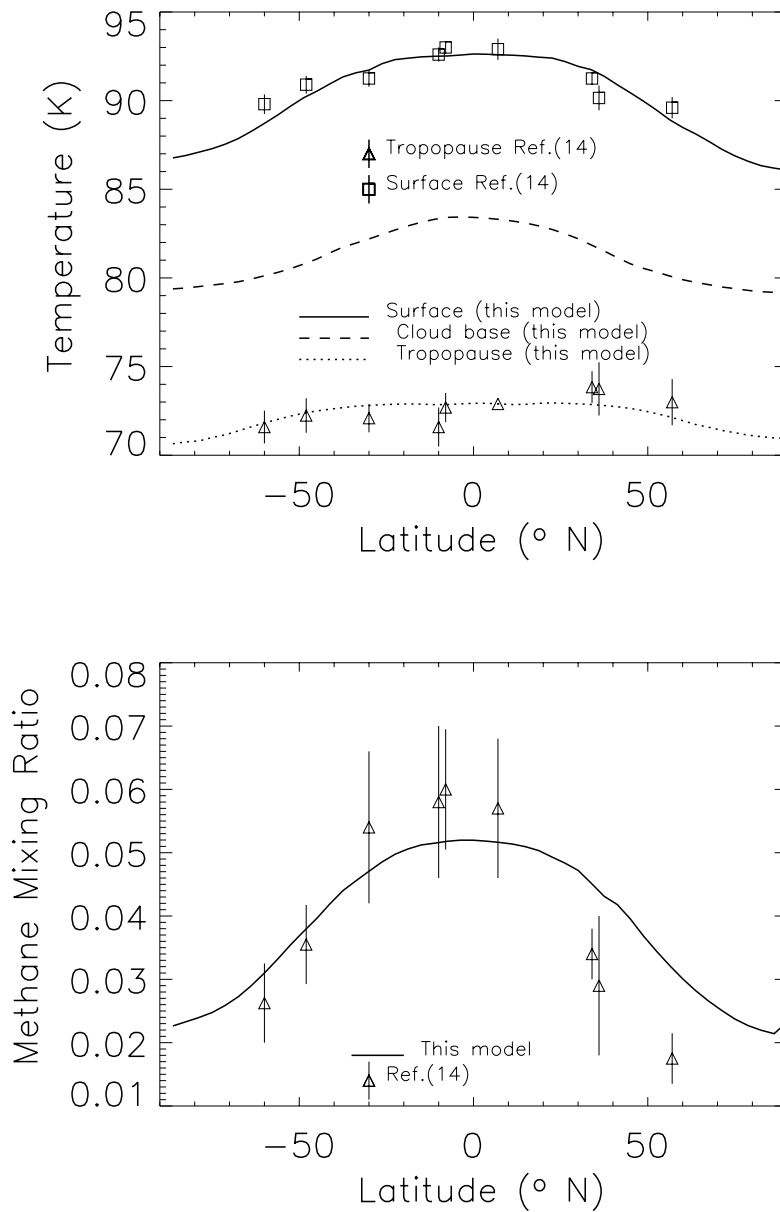


Figure S2 Upper panel: predicted temperature at three levels in the troposphere, compared with temperature inferred from IRIS infrared spectrometer on board Voyager (9). For comparison, the temperature measured by HASI onboard Huygens, at latitude $12^{\circ}S$, is 93.5K at the surface and 70 K at the tropopause (10). Bottom panel: Surface methane mole fraction in our model and inferred from IRIS/Voyager (9). The mole fraction measured by GCMS onboard Huygens is $4.92 \cdot 10^{-2}$ (11).

References

1. Rannou, P., Hourdin, F. & McKay, C.P. A wind origin for Titan's haze structure. *Nature* (2002)
2. Hourdin, F. *et al.* Numerical simulation of the general circulation of the Titan. *Icarus* **117**, 358-374 (1995).
3. Luz, D. and Hourdin, F. Latitudinal transport by barotropic waves in Titan's stratosphere. I General properties from a shallow-water model *Icarus* **166**, 328-342 (2003).
4. Rannou, P., Hourdin, F., McKay, C.P. & Luz, D. A coupled dynamics-microphysics model of Titan's atmosphere. *Icarus* **170**, 443-462 (2004).
5. Montmessin, F., Forget, F., Rannou, P., Cabane, M. & Haberle, R.M. Origin and role of water ice clouds in the Martian water cycle as inferred from a general circulation model. *J. Geoph. Res.* **109** E10, doi: 10.1029/2004JE002284 (2004).
6. Pruppacher, H.R. & Klett, J.D. Microphysics of clouds and precipitation. *Reidel Publishing Company, Dordrecht* (1978).
7. Quirico, E. & Schmitt, B. Near-infrared spectroscopy of simple hydrocarbons and carbon oxides diluted in solid N₂ and as pure ices: implication for Triton and Pluto *Icarus* **127**, 354-378 (1997).
8. Khare, B.N. *et al.* Optical constants of organic tholins produced in a simulated Titanian atmosphere: from soft X-ray to microwave frequencies. *Icarus* **60**, 127-137 (1984).
9. Samuelson, R.E., Nath, N.R. & Borysow, A. Gaseous abundances and methane supersaturation in Titan's troposphere. *Planet. Space Sci.* **45**, 959-980 (1997).
10. Fulchignoni *et al.* HASI Experiment to Titan *Bull. Am. Astron. Soc.* **37** 621 (2005).
11. Niemann *et al.* Results from the Gas Chromatograph Mass Spectrometer (GCMS) Experiment on the Cassini-Huygens Probe. *Bull. Am. Astron. Soc.* **37** 621 (2005).
12. McKay, C.P., Pollack, J.B., and Courtin, R.
The thermal structure of Titan's atmosphere. *Icarus* **80**, 23-53 (1989).
13. Moses, J.I., Allen, M., and Yung, Y.L. Hydrocarbon nucleation and aerosol formation in Neptune's atmosphere *Icarus* **99**, 318-346 (1992).
14. Reid, R.C., Prauznitz, J.M. & Poling, B.E. The properties of gases and liquids. Fourth edition. *McGraw-Hill, New-York* (1987).
15. Barth, E.L. & Toon, O.B. Microphysical modeling of ethane ice clouds in Titan's atmosphere. *Icarus* **162**, 94-113 (2004).

Model parameters and laws			
Surface parameters		Notes	
	Visible albedo 0.2	From (12)	
	Infrared emissivity 1	From (12)	
	Thermal inertia $2000 \text{ Jm}^{-2}\text{s}^{-0.5}\text{K}^{-1}$	From (2)	
Atmosphere parameters		Notes	
Thermal conductivity	$\lambda_{N_2} = 4.184 \times 10^{-3}(2.857 \times 10^{-2}T - 0.5428)$	T temperature	
N_2 molecule radius ¹	$1.75 \times 10^{-10} \text{ m}$	N_2 atmosphere at 95%	
		Notes	
	Methane	Ethane	
Gas sources	Global surface flux Φ_{CH_4} $= \rho_a C_d V_*(q_1 - \alpha q_s(T_s))$	Mass production rate $6 \times 10^{-12} \text{ kg/m}^2/\text{s}$ model top layer	ρ_a Atmosphere density C_d Drag coefficient V_*, q_1 Friction velocity and humidity near surface $q_s(T_s)$ Saturation humidity at surface $\alpha=0.5$
Mass density ¹	425 kg/m^3	544.6 kg/m^3	
Molecule radius ¹	$2 \times 10^{-10} \text{ m}$	$2.22 \times 10^{-10} \text{ m}$	
Mole volume ¹	$3.76 \times 10^{-5} \text{ m}^3/\text{mol}$	$5.47 \times 10^{-5} \text{ m}^3/\text{mol}$	
Desorption enthalpy	$2.88 \times 10^{-20} \text{ J/molec}$	$2.88 \times 10^{-20} \text{ J/molec}$	From (13)
Jump frequency	10^{13} s^{-1}	10^{13} s^{-1}	From (13)
Contact angle	0.97	0.97	Aerosols wetted by nitriles
Pressure vapor ¹	$\ln P_s/P_c = \frac{aT' + bT'^{1.5} + cT'^3 + dT'^6}{1-T'}$ with $T' = 1 - T/T_c$, the critical temperature T_c P_c the critical pressure $a = -6.00435$ $a = -6.34307$ $b = 1.18850$ $b = 1.011630$ $c = -0.83408$ $c = -1.19116$ $d = -1.22833$ $d = -2.03539$ $P_c = 46 \times 10^5 \text{ Pa}$ $P_c = 48.8 \times 10^5 \text{ Pa}$ $T_c = 190.4 \text{ K}$ $T_c = 305.5 \text{ K}$		Eq (7-5.2) (14)
Vapor latent heat ¹	$\frac{\Delta H}{RT_c} = 7.08T'^{0.354} + 10.95\omega T'^{0.456}$ Where ΔH is the latent heat, R the ideal gas constant, $T' = 1 - T/T_c$, the critical temperature T_c $\omega = 1.1 \times 10^{-2}$ $\omega = 9.9 \times 10^{-2}$		Eq (7-9.4) (14)
Surface tension ^{1,2}	$\sigma = 10^{-3}(T/4 + 41.)$	$\sigma = 21.157(\frac{305.42-T}{305.42-153.2})^{11/9}$	

¹ Derived from molecular theory (14)

² From (15)

TABLE S1